J Wood Sci (2000) 46:273–278

ORIGINAL ARTICLE

Hiroshi Yoshihara · Masamitsu Ohta

Measurement of mode II fracture toughness of wood by the end-notched flexure test

Received: June 21, 1999 / Accepted: September 3, 1999

Abstract We examined the applicability of end-notched flexure (ENF) tests for measuring the mode II fracture toughness of wood. Western hemlock (*Tsuga heterophylla* Sarg.) was used for the specimens. The fracture toughness at the beginning of crack propagation G_{IIc} and that during crack propagation G_{IIR} were calculated from the load-loading point compliance and load-crack shear displacement (CSD) relations. The obtained results were compared with each other, and the validity of measurement methods were examined. The results are summarized as follows: (1) The value of G_{IIc} increased with the increase in initial crack length. When measuring G_{IIc} by ENF tests, we should be aware of the dependence of G_{IIc} on the initial crack length. (2) The value of G_{IIR} initially increased with the crack length, and it reached a constant value. (3) Measurement of the CSD is recommended when obtaining G_{IIR} because the crack length, which has a great influence on the G_{IIR} calculation, is implicitly included in the CSD. (4) We found that the crack length during its propagation should be evaluated by the final crack length.

Key words Fracture toughness · Mode II · ENF test · CSD gauge

Introduction

In linear-fracture mechanics, an in-plane shear mode fracture is defined as a "mode II" fracture; and the mode II fracture behaviors of wood had been variously analyzed.[1–7] Recently, a draft standard for measuring the mode II fracture toughness was proposed by the International Union of Testing and Research Laboratories for Materials and Structures (RILEM).[7] Nevertheless, the specimen shape in the draft is complicated, and we are afraid that the proposed method cannot become popular.

Among the various mode II fracture testing methods, the end notched flexure (ENF) test is frequently used for fiber-reinforced composites, and testing techniques have been developed during the past two decades.[8–13] We thought that these experimental techniques might be applied to measurement of the mode II fracture toughness of wood. Here, we examined the validity of the ENF testing method for measuring the mode II fracture toughness of wood.

Theory

Energy release rate derived by ENF test

Russell and Street derived an equation that gives the mode II energy release rate by ENF test.[8] As shown in Fig. 1, an ENF specimen with the crack length of a is loaded by P at the center of the span of $2L$. In this case, the equation of bending is given by the elementary beam theory as follows.

$$\begin{cases} \dfrac{E_x I}{8}\dfrac{d^2y}{dx^2} = -\dfrac{1}{4}Px & (0 \le x \le a) \\ E_x I\dfrac{d^2y}{dx^2} = -\dfrac{1}{2}Px & (a \le x \le L) \\ E_x I\dfrac{d^2y}{dx^2} = \dfrac{1}{2}Px - PL & (L \le x \le 2L) \end{cases} \quad (1)$$

where E_x is Young's modulus in the longitudinal axis, and I is the second moment of cross-sectional area in the crack-free region. Solving this equation, we can obtain the displacement at the loading point, v, as follows.

$$v = \frac{P\left(2L^3 + 3a^3\right)}{12E_x I} \quad (2)$$

H. Yoshihara (✉)
Faculty of Science and Engineering, Shimane University,
1060 Nishikawazu-cho, Matsue, Shimane 690-8504, Japan
Tel. +81-852-32-6508; Fax +81-852-32-6598
e-mail: yosihara@riko.shimane-u.ac.jp

M. Ohta
Graduate School of Agricultural and Life Sciences, The University of Tokyo, Bunkyo-ku, Tokyo 113-8657, Japan

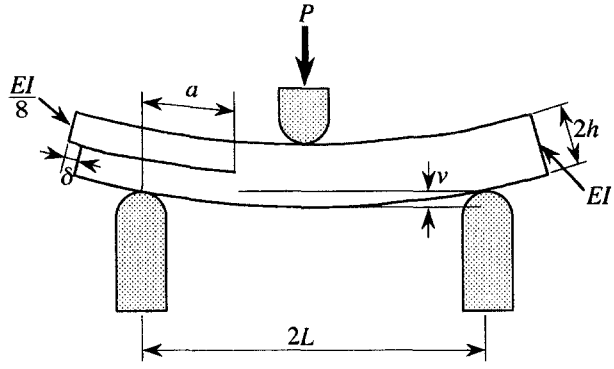

Fig. 1. End noched flexure (ENF) test

The loading point compliance C is defined as follows:

$$C = \frac{v}{P} = \frac{2L^3 + 3a^3}{12E_xI} \tag{3}$$

The energy release rate, G_{II}, is given as:

$$G_{II} = \frac{P^2}{2b}\cdot\frac{dC}{da} \tag{4}$$

where b is the width of the beam. By substituting Eq. (3) into Eq. (4), the energy release rate can be written as:

$$G_{II} = \frac{9CP^2a^2}{2b\left(2L^3 + 3a^3\right)} \tag{5}$$

Another equation for the energy release rate was given by Kageyama and colleagues.[10] The crack shear displacement (CSD) δ, which is defined in Fig. 1, is obtained by integrating the strain along the longitudinal axis from the lower end corner of the upper beam to the crack tip; it is given as follows.

$$\delta = 2\int_0^a \frac{h}{2E_xI'}Mdx = \frac{h}{E_xI'}\int_0^a \frac{Px}{4}dx = \frac{ha^2}{8E_xI'}P \tag{6}$$

where h is the upper beam height of cracked region, I' is the second moment of cross-sectional area in the cracked region (which equals $I/8$), and M is the bending moment. The compliance λ in this case is written as follows:

$$\lambda = \frac{\delta}{P} = \frac{ha^2}{8E_xI'} \tag{7}$$

From Eqs. (3), (5), and (7), the energy release rate can be formulated without the crack length as:

$$G_{II} = \frac{P^2}{2b}\cdot\frac{dC}{da} = \frac{P^2}{2b}\cdot\frac{3a^2}{4E_xI} = \frac{3}{8}\cdot\frac{P\delta}{bh} = \frac{3}{8}\cdot\frac{P^2\lambda}{bh} \tag{8}$$

Stability of crack propagation

The stability of crack propagation is evaluated by the sign of dG_{II}/da. Under the constant loading point displacement condition, dG_{II}/da is derived from Eqs. (4) and (6) as follows.[10]

$$\frac{dG_{II}}{da} = \frac{3v^2a}{4E_xIbC^2}\left(1 - \frac{9a^3}{2L^3 + 3a^3}\right) \tag{9}$$

When the value of dG_{II}/da is negative, the crack propagation is stable. Then the fracture toughness during the crack propagation can be obtained when the crack length satisfies the following relation.

$$a \geq \frac{L}{\sqrt[3]{3}} \approx 0.7L \tag{10}$$

Otherwise, the crack grows unstably, and only the fracture toughness at the beginning of crack propagation can be obtained.

Experiment

Materials

Western hemlock (*Tsuga heterophylla* Sarg.) whose density of 0.48 g/cm^3 was used for the specimens. Specimens were conditioned at 20°C and 65% relative humidity (RH) before and during the tests.

ENF tests

A beam specimen was cut with the dimensions of 20 mm (radial direction) × 20 mm (tangential direction) × 500 mm (longitudinal direction). The crack was produced in the longitudinal-tangential plane, which is the so-called TL system.[1] The crack, with the thickness of 1 mm, was first cut by a band saw and then was extended by a razor blade. The initial crack length a_0 varied from 69 to 207 mm at intervals of 23 mm. This range corresponded to the value of a_0/L from 0.3 to 0.9 at intervals of 0.1. Two sheets of Teflon film with 0.5 mm thickness were inserted between the crack surfaces to reduce the friction between the upper and lower cantilever beams. This specimen was supported with the span of 460 mm, and a load was applied at the center of the spans at the crosshead speed of 2 mm/min.

The loading point displacement v was measured by a dial gauge set below the loading nose, whereas the crack shear displacement δ was measured by the CSD gauge set on the upper cantilever of the specimen as in Fig. 2. As shown in Fig. 3, the "critical load" P_c was determined as the load of the intersection point between the two straight-line segments through the pre- and postlinear portions of the load-loading point displacement or load-CSD curves.

The fracture toughness at the beginning of crack propagation G_{IIc} was calculated for every specimen from Eqs. (5) and (8). For the specimen whose a_0/L was 0.7 or 0.8, the fracture toughness during the crack propagation G_{IIR} was also obtained because the crack propagation was stable and the crack path was long enough in this initial crack length

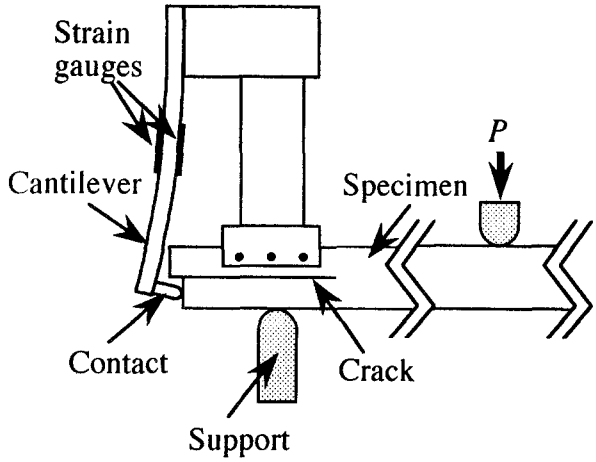

Fig. 2. Crack shear displacement (CSD) gauge

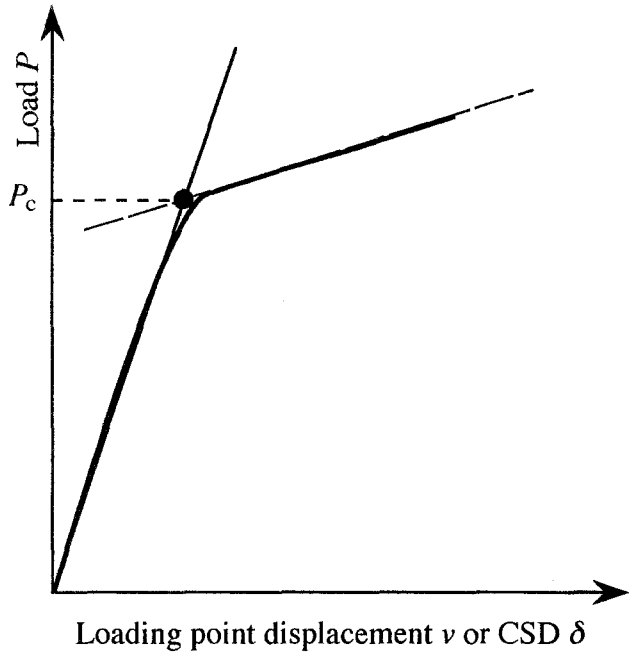

Fig. 3. Determination of the critical load P_c

range. Prior to the tests, straight lines were drawn in the crack-free region of an LT plane at intervals of 5mm perpendicular to the crack. A load was applied until a marker line split. This process was performed under a magnifying glass. The specimen was then unloaded until a certain load was attained, and the crack length was measured again because the crack opened a little during the unloading. The specimen was then reloaded until another 5-mm crack appeared. This load–unload process was repeated, and the value of G_{IIR} corresponding to each crack length was obtained.

In ENF test, the crack propagates without a clear opening, and it is difficult to measure the propagating crack precisely. Therefore, we tried to estimate the crack length by the following five equations. From Eq. (5), the propagating crack length a_p is derived as:[8]

$$a_p = \left[\frac{C_p}{C_0}a_0^3 + \frac{2}{3}\left(\frac{C_p}{C_0} - 1\right)L^3\right]^{\frac{1}{3}} \tag{11}$$

where a_0 and C_0 are the initial crack length and the initial loading point compliance, respectively; and C_p is the loading point compliance during crack propagation. Similarly, a_p is derived by the final crack length a_f and loading point compliance C_f as follows.

$$a_p = \left[\frac{C_p}{C_f}a_f^3 + \frac{2}{3}\left(\frac{C_p}{C_f} - 1\right)L^3\right]^{\frac{1}{3}} \tag{12}$$

From Eq. (7), a_p is derived as:

$$a_p = a_0\sqrt{\frac{\lambda_p}{\lambda_0}} \tag{13}$$

where λ_0 and λ_p are the load-CSD compliances at the initial and during the crack propagation, respectively. Similarly, a_p is derived by the final crack length a_f and the CSD compliance λ_f as:

$$a_p = a_f\sqrt{\frac{\lambda_p}{\lambda_f}} \tag{14}$$

Another equation, proposed by Kageyama and colleagues, is shown as follows.[12]

$$a_p = 2h\left(\beta_0 + \beta_1\sqrt{b\lambda}\right) \tag{15}$$

where

$$\beta_0 = -\frac{1}{2}\sqrt{\frac{1}{62.4}\left(\frac{E_x}{G_{xy}}\right)\left\{3 - 2\left(\frac{\sqrt{E_xE_y}}{4.8G_{xy} + \sqrt{E_xE_y}}\right)\right\}^2} \tag{16}$$

and

$$\beta_1 = \sqrt{\frac{E_x}{6}} \tag{17}$$

where E_y is Young's modulus in the direction of thickness, and G_{xy} is the shear modulus. The values of E_x, E_y, and G_{xy} were determined by compression tests (see below).

Compression tests

To determine the values of β_0 and β_1 in Eq. (15), we measured Young's moduli E_x and E_y and the shear modulus G_{xy} by compression tests. Short-column specimens whose dimensions were 40 × 20 × 20mm were prepared. When measuring E_x and E_y, the long axis of the specimen coincided with the longitudinal and tangential directions of wood, respectively; whereas when measuring G_{xy}, the long axis coincided with the direction inclined at 45 degrees with respect to the grain. Strain gauges were bonded at the centers of the LT planes; and from the stress-strain relation,

Young's moduli were obtained. The shear modulus were determined from the following equation.

$$G_{xy} = \frac{E_{45}}{2(1 + \nu_{45})} \tag{18}$$

where E_{45} and ν_{45} are Young's modulus and Poisson's ratio in the direction inclined at 45 degrees with respect to the grain, respectively.

Results and discussion

Fracture toughness at the beginning of crack propagation

Figure 4 represents the fracture toughness at the beginning of crack propagation G_{IIc} corresponding to the initial crack length a_0. The value of G_{IIc} increased with the increase of the initial crack length a_0 whether the compliance was determined from the loading point displacement or CSD. Hence, we believe that the value of G_{IIc} should be reported with the initial crack length as an important testing condition.

Fracture toughness during the crack propagation

Figure 5 shows examples of the load-loading point displacement and load-CSD relations. For the ENF tests of brittle epoxy material, a maximum load can be observed in one load-unload procedure.[8] In our experiment, the load did not decrease during crack propagation.

Figure 6 presents examples of fracture toughness during the crack propagations G_{IIR} corresponding to the crack propagation length Δa. The fracture toughness of brittle material tends to be constant even during the early stage of crack propagation.[11] In contrast, it is reported that in materials with irregular fiber distribution a bridging between the crack surfaces occurs; the crack propagation is interrupted by this "fiber bridging," and the G_{IIR} increases with crack propagation (K. Kageyama, personal communication, 1999). In our experiment, the value of G_{IIR} reached a constant value when the crack grew to more than 200 mm. The representative value of G_{IIR}, which is denoted as $\overline{G_{IIR}}$, was then defined as the average of the data obtained from the >200 mm crack length region. Table 1 shows the values of $\overline{G_{IIR}}$ obtained from the load-loading point compliances and load-CSD compliance relations. We think that the value of $\overline{G_{IIR}}$ varies by the estimation method, and that the method for determining $\overline{G_{IIR}}$ should be examined furthermore. As mentioned by Tanaka and colleagues, it may be advantageous to evaluate fracturing behavior from the whole relation between fracture toughness and crack propagation length.[11]

Table 1. Representative value of fracture toughness during crack propagation, $\overline{G_{IIR}}$

a_0/L	Measurement of compliance (kJ/m^2)	
	Loading point compliance	Crack shear displacement
0.7	0.61 ± 0.13	0.68 ± 0.11
0.8	0.67 ± 0.27	0.71 ± 0.11

Results are the average ± SD

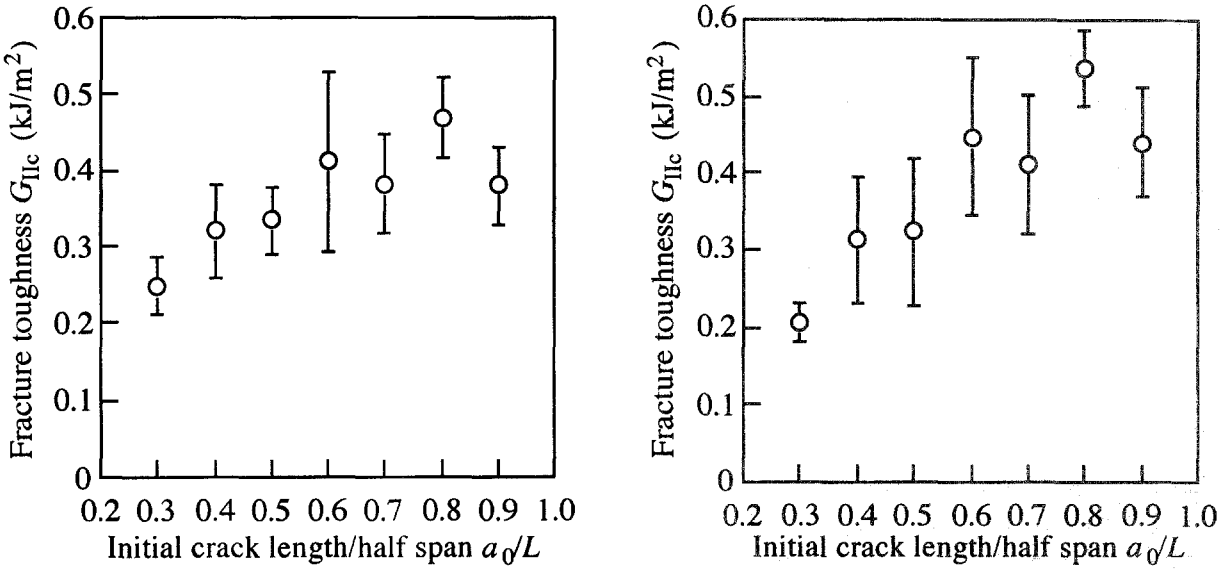

Fig. 4. Fracture toughness at the beginning of crack propagation G_{IIc} corresponding to the initial crack length/half span. *Circles* and *horizontal bars* represent the mean and standard deviations, respectively. Fracture toughness was calculated from the loading point compliance (**left**) and the CSD compliance (**right**)

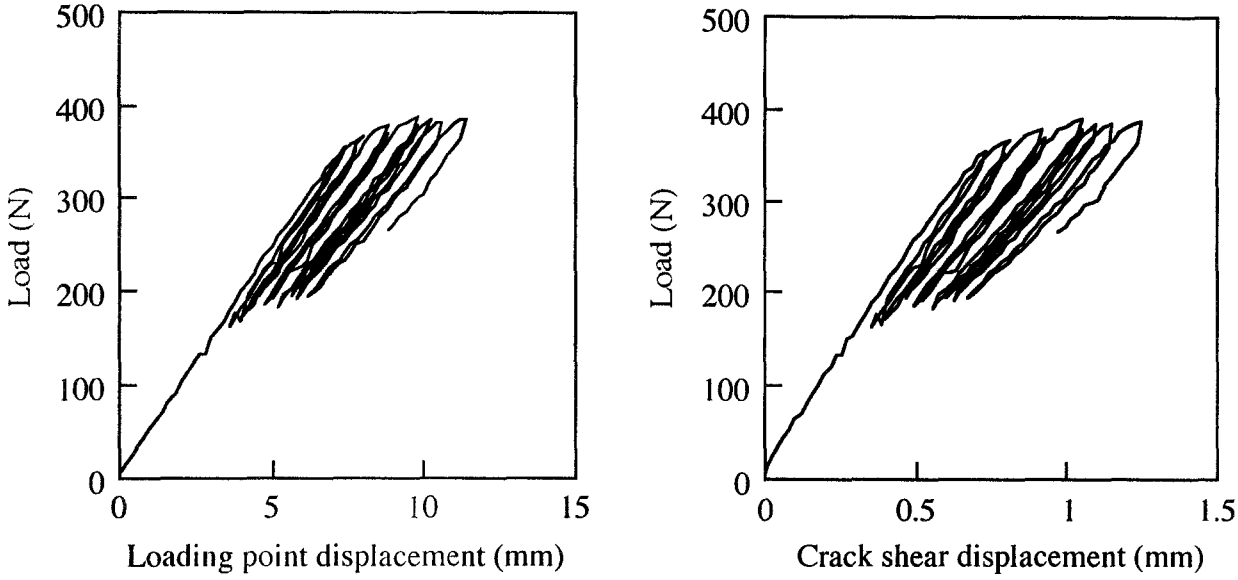

Fig. 5. Examples of the records of the load–unload process. Initial crack length/half span was 0.7

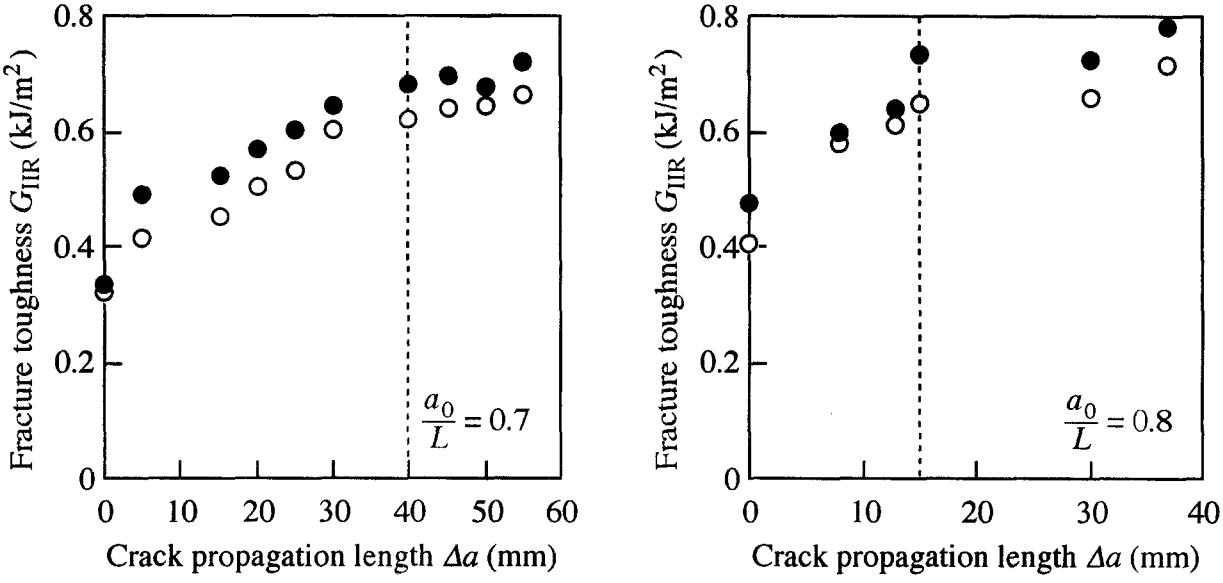

Fig. 6. Changes in the fracture toughness G_{IIR} during crack propagation. *Open circles* and *solid circles* were obtained from the loading point compliances and CSD compliances, respectively; *dashed line* represents the overall crack length of 200 mm

When calculating fracture toughness from the load-CSD relation, the crack length is implicitly included in the CSD compliance λ, and we can obtain the value of G_{IIR} without measuring the crack length. Considering the difficulty of monitoring the propagating crack length, CSD measurement is recommended for obtaining the fracture toughness G_{IIR}. Additionally, the crack can propagate stably when the CSD is controlled to increase at a constant rate.[10,11,13] In our experiment, however, this "CSD control method" could not be used because our testing machine was incapable of such measurement. In the future, the "CSD control method" should be examined for obtaining details of the mode II fracture behaviors of wood.

Measurement of crack length

To evaluate the crack length by the equation proposed by Kageyama and colleagues, Eq. (15), we used values of 12.3, 0.80, and 1.18 GPa for E_x, E_y, and G_{xy}, respectively. Figure 7 shows a comparison between the calculated and observed crack lengths. The crack length calculated by Eqs. (11) and (13), which contains the initial crack length and compliances, deviated from the observed crack length even during an early stage. In contrast, when using the final crack length and compliances, the crack length calculated by Eqs. (12) and (14) were closer to the observed one when the crack length was long enough. The latter tendency was also

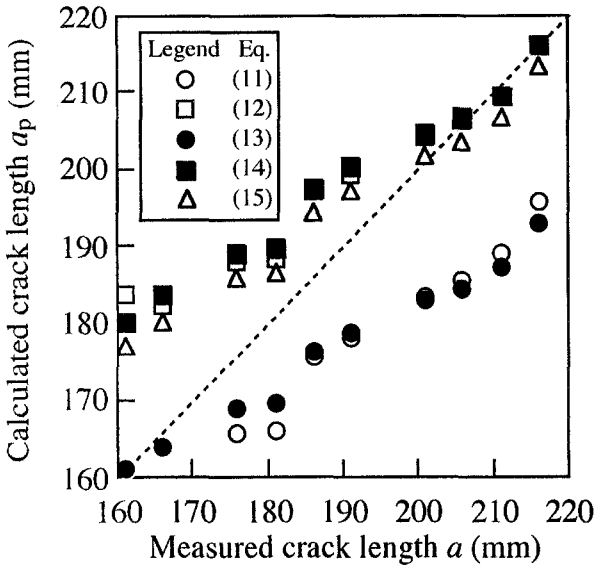

Fig. 7. Comparison of the predicted and measured crack lengths. Initial crack length/half span was 0.7

found in the results obtained from Eq. (15), proposed by Kageyama and colleagues; and the coincidence was good in the crack length range where G_{IIR} was a constant value. Considering the difficulty of measuring the propagating crack length, we recommend that it be evaluated by means of the final crack length.

Conclusions

We measured the mode II fracture toughness of wood by end-notched flexure tests, and following results were obtained.

1. The fracture toughness at the beginning of crack propagation G_{IIc} increased with the increase of the initial crack length. Hence, we should consider the dependence of the fracture toughness on the initial crack length.

2. The fracture toughness during the crack propagation G_{IIR} initially increased and was close to a constant value.

3. Measurement of CSD is recommended when obtaining G_{IIR} because the crack length, which has a serious influence on the calculation of G_{IIR}, is implicitly included in the CSD.

4. We recommend that the crack length during propagation be evaluated based on the final crack length.

Acknowledgments We thank Prof. Kazuro Kageyama at The University of Tokyo, Prof. Peer Haller at The Dresden Technical University, and Mr. Koji Nagaoka, a graduate student of The University of Tokyo, for their advice and help in conducting our experiment. This research was supported partly by a Grant-in-Aid for Scientific Research (09460072) from the Ministry of Education, Science and Culture of Japan.

References

1. Barrett JD, Foschi RO (1977) Mode II stress-intensity factors for cracked wood beams. Eng Fract Mech 9:371–378
2. Cramer SM, Purge AD (1987) Compact shear specimen for wood mode II fracture investigations. Int J Fract 35:163–174
3. Murphy JF (1988) Mode II wood test specimen: beam with center slit. J Test Eval 16:364–368
4. Prokopski G (1995) Investigation of wood fracture toughness using mode II fracture (shearing). J Mater Sci 30:4745–4750
5. Stanzl-Tschegg SE, Tan DM, Tschegg EK (1996) Mode II fracture tests on spruce wood. Mokuzai Gakkaishi 42:642–650
6. Xu S, Reinhardt HW, Gappoev M (1996) Mode II fracture testing method for highly orthotropic materials like wood. Int J Fract 75:185–214
7. Aicher S, Boström L, Gierl M, Kretschmann D, Valentin G (1997) Determination of fracture energy of wood in mode II. RILEM TC 133 report
8. Russell AJ, Street KN (1985) Moisture and temperature effects on the mixed-mode delamination fracture of unidirectional graphite/epoxy. ASTM STP 876:349–370
9. Gillespie JW Jr, Carlsson LA, Pipes RB (1986) Finite element analysis of the end notched flexure specimen for measuring mode II fracture toughness. Comp Sci Technol 27:177–197
10. Kageyama K, Kikuchi M, Yanagisawa N (1991) Stabilized end notched flexure test: characterization of mode II interlaminar crack growth. ASTM STP 1110:210–225
11. Tanaka K, Kageyama K, Hojo M (1995) Prestandardization study on mode II interlaminar fracture toughness test for CFRP in Japan. Composites 26:257–267
12. Williams JG (1989) The fracture mechanics of delamination tests. J Strain Anal 24:207–214
13. Li Z-W, Kimpara I, Kageyama K, Suzuki T, Ohsawa I (1997) Testing method for evaluation of mode II fatigue delamination growth behaviors of advanced composite materials by applying CSD measurement (in Japanese). Trans Jpn Comp Mater 23:92–99